Gold-free Tantalum and Titanium-based Ohmic Contacts for Gallium Nitride HEMT Devices

Gareth Davies[1], Andrew Withey[2], O. J Guy[3], Jon E. Evans[3], Mike Jennings[3]
[1]Swansea University, Bay Campus, Crymlyn Burrows, Skewen, Swansea SA18EN, 2152949@swansea.ac.uk
[2]Vishay Ltd, Tower House, St Catherine's Court, Sunderland, SR53XJ
[3]Centre for Integrative Semiconductor Materials (CISM), Bay Campus, Crymlyn Burrows, Skewen, Swansea SA18EN

Keywords: Gold-free, AlGaN, HEMT, Thermionic Field Emission, Specific Contact Resistance

Abstract

This study aims to optimise the performance of metal-semiconductor contacts through an analysis of six Al/GaN semiconductor material variations, focusing on GaN/AlGaN thicknesses, AlN substrates, and carbon doping concentrations. From these six wafers, three will be subjected to mechanical and electrical testing. The research endeavors to evaluate the viability of gold-free tantalum and titanium contacts and to gain insights into the current transport mechanisms for ohmic contacts. To measure the specific contact resistivity at varying temperatures contacts were fabricated using pure Al, AlSiCu, Ti, and Ta. The lowest ρ_C was measured on titanium-based ohmic contacts in the region of 10^{-3} Ωcm^2. All ohmic contacts measured demonstrated resistivities in the range of 10^{-1} – 10^{-3} Ωcm^2. Moreover, we demonstrate that the structural integrity of the contact following a 600°C annealing process, remained intact (SEM). The current transport mechanism analysis for the Al-based contacts a barrier height (Φ_B) of 0.66eV. A similar result was obtained for pure Ti-based ohmic contacts with all displaying the thermionic field emission current transport mechanism.

INTRODUCTION

The growing interest in wide bandgap semiconductors, such as gallium nitride (GaN) and silicon carbide (SiC), for power electronics is attributable to their high energy efficiency. In the realm of energy processes, power electronics holds a pivotal position, with projections indicating that approximately 80% of electrical energy will pass through such systems by 2030 [1-2]. While silicon has long been dominant, the quest for nearly 100% energy efficiency and compact designs has fueled the emergence of GaN. GaN, with its wide bandgap, stands as a promising candidate for high-power and high-temperature applications, particularly in the realm of power electronics [3]. Moreover, aluminum nitride (AlN), another wide bandgap semiconductor, shares comparable electronic and optical properties with GaN, enabling their combined utilisation in various electronic devices, including high-power transistors, microwave devices and sensors. For instance, in high-electron-mobility transistors (HEMTs), GaN serves as the active layer, while the implementation of AlN, with its superior thermal conductivity, promotes effective heat dissipation, thereby enhancing power density and overall device performance [4]. The quality of metal contacts holds pivotal importance in determining the overall performance of these devices. Ohmic contacts facilitate efficient carrier injection and extraction at the transistors source and drain terminals, thereby facilitating electron transport across the channel region. Attaining low contact resistivity is crucial for minimising power losses and maximising device efficiency. The intricate interplay between the properties of the contact material, the semiconductor and the fabrication processes significantly influences contact resistance, subsequently impacting the device's current transport mechanisms. In light of these considerations, this study conducts a comprehensive evaluation of pure aluminum (Pure Al), aluminum silicon copper (AlSiCu), tantalum (Ta), and titanium (Ti) ohmic contacts on GaN-based HEMTs, with electrical data extracted at temperatures ranging from 300K to 400K. The study aims to elucidate the key factors influencing contact resistivity, their influence on current transport, and their overall significance in determining device functionality.

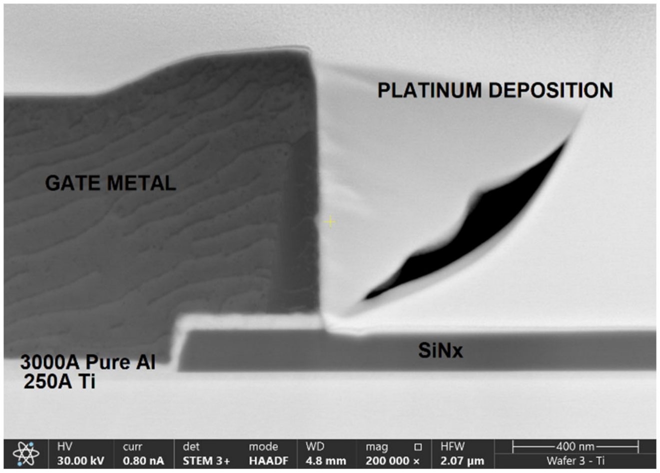

Fig. 1. TEM image of TLM contact 250ÅTi / 3000Å Pure Al

DEVICE DETAILS

For the wafers analysed, the GaN layers and AlGaN/GaN heterostructures investigated in this study were carefully grown on CZ p-type Si (111) substrates. The growth process utilised trimethylgallium, trimethylaluminum, and ammonia as precursors for gallium, aluminum, and nitrogen, respectively. A detailed breakdown of the layer composition is provided in Tables 1 and 2. For three wafers the nucleation process was used to initiate the growth of Gallium Nitride crystals as shown in Table 1. And for the other three wafers, an AlN buffer was precisely deposited, followed by a single thick AlGaN intermediate layer and a substantial GaN layer, as illustrated in Table 2.

Layer	Type	Material	Mole Fraction (x)	Thickness [nm]	Dopant
5	UID	GaN	-	3	-
4	UID	Al(x)GaN	25%	28	-
3	UID	GaN	-	400	-
2	SI	GaN/AlGaN buffer	-	3650	carbon
1	UID	Nucleation	-	180	-
CZ Si (111) p-type (1150000nm)					

Table 1. The GaN nucleation epi wafer structure studied in this work.

Layer	Type	Material	Mole Fraction (x)	Thickness [nm]	Dopant
7	UID	GaN	-	3	-
6	UID	Al(x)GaN	25%	20	-
5	UID	AlN	-	0.5	-
4	UID	GaN	-	400	-
3	SI	GaN	-	900	carbon
2	SI	GaN/AlGaN buffer	-	2750	carbon
1	UID	AlN	-	180	-
CZ Si (111) p-type (1150000nm)					

Table 2. The GaN AlN epi wafer structure studied in this work.

This strategic layering process is crucial to the fabrication of the GaN-based HEMTs under investigation, contributing to the structural and electronic properties that are integral to the performance of the ohmic contacts. These device details lay the foundation for the subsequent analysis, providing insight into the specific materials and growth processes employed in the creation of the GaN layers and AlGaN/GaN heterostructures (Fig. 2). The information presented here establishes the context for the subsequent examination of the ohmic contacts and their impact on the overall functionality of the devices.

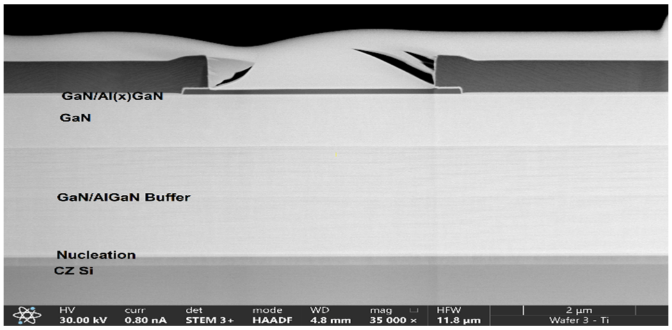

Fig. 2. TEM image of the nucleation GaN epi

FABRICATION

The fabrication process for creating PCM (TLM) structures (Fig. 3) in semiconductor manufacturing adheres to a particularly orchestrated four-mask sequence. Commencing with mask 1, a 140nm LPCVD nitride layer is uniformly patterned using the TEL mark8 coater and developer.

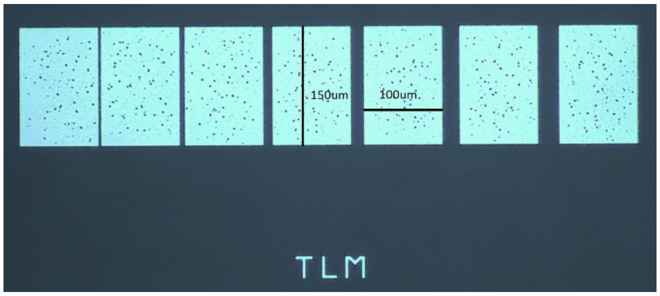

Fig. 3. Optical image showing fabricated TLM structures of 150µm x 100µm with incremental spacings of 2µm, 5µm, 10µm, 15µm, 20µm and 25µm.

Subsequently, alignment marks are precisely exposed via a photo stepper in the zero-photo step, followed by etching of the nitride layer to a depth of approximately 500nm into GaN. This intricate etching process is executed using ICP and DPS tools in the zero etch step. In the subsequent ohmic window photo step, specific areas, including the source/drain regions, are exposed using the photo stepper. Advancing to mask 2, the oxide layer within the source/drain regions undergoes controlled etching through ICP in the ohmic window etch step. The pre-metal clean step involves O_2 ash and DSP cleaning. Metal deposition is then carried out, utilising either Ti/Al or Ta/Al through the AMAT Endura tool in the metal deposition step. To enhance the electrical properties of the metal contacts, ohmic annealing is performed via RTP. Subsequently, another round of pre-metal cleaning is executed before the final metal deposition as shown in Table 3. Transitioning to mask 3, the metal layer is patterned through exposure with a photo stepper in the metal photo step. Unwanted metal layers are selectively etched using DRIE (Deep Reactive Ion Etch) in the metal etch step. Moving on to mask 4, isolation regions are exposed via a photo stepper in the isolation photo step. Isolation implantation is then carried out through the GSD tool. The process concludes with isolation stripping, achieved through O_2 ash and DSP cleaning.

Epi	Ohmic Metal	Total Thickness (Å)	Max Ohmic Anneal
Nucleation, GaN/AlGaN buffer & GaN	400ÅTa / 2000Å Pure Al	2400	600°C, 60s
Nucleation, GaN/AlGaN buffer & GaN	250ÅTi / 3000Å AlCu	3250	600°C, 60s
Nucleation, GaN/AlGaN buffer & GaN	250ÅTi / 3000Å Pure Al	3250	600°C, 60s
AlN, GaN/AlGaN buffer & GaN	400ÅTa / 2000Å Pure Al	2400	600°C, 60s
AlN, GaN/AlGaN buffer & GaN	250ÅTi / 3000Å AlCu	3250	600°C, 60s
AlN, GaN/AlGaN buffer & GaN	250ÅTi / 3000Å Pure Al	3250	600°C, 60s

Table 3. Summary of stacked metal contacts reported on in this abstract.

RESULTS

Ohmic contacts were fabricated onto the GaN substrate, with the layer composition detailed in Tables 1 and 2. The metallisation and subsequent post-annealing treatments are systematically presented in Table 3. All contacts underwent annealing at a maximum temperature of 600 °C to assess their structural integrity. The SEM image (Fig. 1) provides a visual confirmation of the contact's structural integrity post a 600°C annealing process, highlighting the robustness of the fabrication methodology. Specific contact resistivity (ρ_C) was measured at the centre, mid-radius, and the edge of the wafer at various temperatures for contacts made from pure Al, AlSiCu, Ti, and Ta, with a focus on the temperature profile of 400K (Fig. 4). Notably, the specific contact resistivity values measured at 400K exhibited promising results:

- 400Å Ta / 2000Å Pure Al contact: 1.11×10^{-2} Ωcm^2
- 250Å Ti / 3000Å AlCu contact: 2.96×10^{-3} Ωcm^2
- 250Å Ti / 3000Å Pure Al contact: 3.14×10^{-3} Ωcm^2

These resistivity values are notable, demonstrating an approximate order of magnitude reduction compared to contacts measured at room temperature. This alignment with the classic thermionic emission (TFE) theory underscores the effectiveness of the annealing process in optimising the electrical properties of the contacts. In-depth analysis of the current transport mechanism for Ti-based ohmic contacts (Fig. 5) revealed a doping density (N_D) of 7.7×10^{18} cm^{-3}. This insight into the doping density provides valuable information on the concentration of charge carriers within the semiconductor material, influencing the overall conductivity. Similarly, the TFE analysis for Ti-based ohmic contacts yielded a barrier height (Φ_B) of 0.66eV. This barrier height determination is crucial in understanding the energy barrier that carriers must overcome during transport, impacting the efficiency of charge injection and extraction processes.

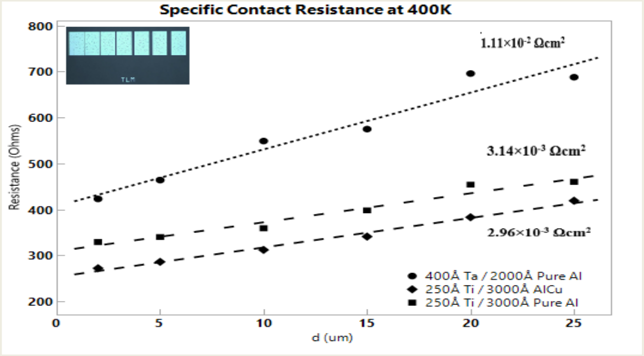

Fig. 4. Specific contact resistance at 400K for 250ÅTi / 3000Å Pure Al and 250ÅTi / 3000Å AlCu and 400ÅTa / 2000Å Pure Al contacts. Inset is the transmission line method (TLM) metallization characterized electrically.

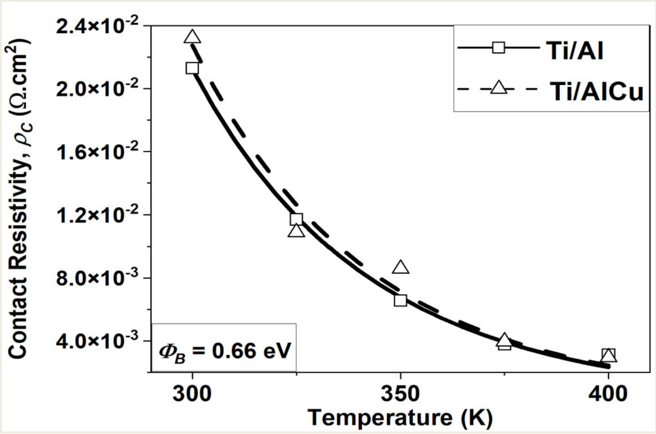

Fig. 5. Typical ohmic contact resistivity vs. temperature profiles (including TFE line fits) for Ti/Al-based contacts showing consistency in terms of thermionic field emission and a barrier height, Φ_B of 0.66 eV.

Top-down SEM images provided visual conformation of zero defectivity. Complementing this technique, Transmission Electron Microscopy (TEM) was employed, providing high-resolution imagery (Fig. 6, 7, and 8) for a thorough examination of the contact's internal structure. TEM was used to detect any anomalies or contamination that could potentially influence the electrical characteristics. The SEM and TEM images, collectively affirmed the absence of defectivity, highlighting the structural robustness of the ohmic contacts. Furthermore, EDX line scan analyses conducted across the contact/GaN interface, utilising elemental mapping provided conclusive evidence of an uncontaminated interface, reinforcing the reliability of the fabricated contacts for subsequent electrical measurements and analyses.

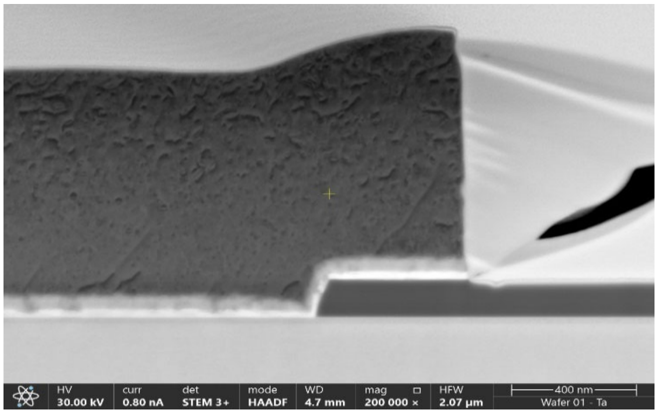

Fig. 6. 400ÅTa / 2000Å Pure Al contact showing TEM lamella across the left side of the contact, GaN interface.

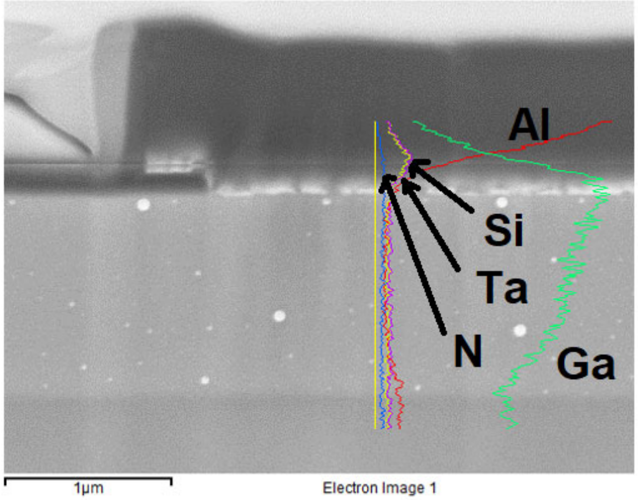

Fig. 7. 400ÅTa / 2000Å Pure Al contact showing the EDX linescan across a FIB of the right side of the contact Al showing, Si, N, Ga, Ta and Al

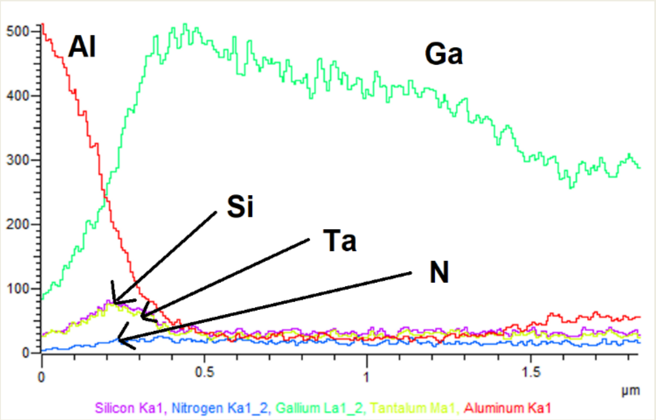

Fig. 8. EDX linescan data across the 400ÅTa / 2000Å Pure Al contact

CONCLUSION

The research explored various material variations, including pure Al, AlSiCu, Ti and Ta, assessing their specific contact resistivity (ρ_C) and current transport mechanisms. The results demonstrated promising outcomes, with specific contact resistivity values at 400K showing an order of magnitude reduction compared to room temperature measurements, aligning with classic thermionic emission (TFE) theory. The structural integrity of the contacts, confirmed through SEM images post a 600°C annealing process, underscores the robustness of the fabrication methodology. Noteworthy findings include the low specific contact resistivity achieved with titanium-based ohmic contacts and the detailed analysis of the current transport mechanism, revealing a doping density (N_D) of 7.7×10^{18} cm^{-3} and a barrier height (Φ_B) of 0.66eV. Future work is suggested to further explore material variations, temperature dependencies, device geometries, and advanced characterization techniques, ensuring a continuous refinement of ohmic contacts for GaN-based HEMT devices. Overall, this research contributes valuable insights to the field of semiconductor manufacturing and power electronics, offering a foundation for advancements in device design and performance optimisation.

ACKNOWLEDGEMENTS

The author would like to thank Professor Mike Jennings and Doctor Andrew Withey for their continued support. Thanks, must also go to the assistance received from the fabrication team that helped process the wafers through the clean room.

REFERENCES

[1] Roccaforte, F.; Greco, G.; Fiorenza, P.; Iucolano, F. *An Overview of Normally Off GaN-Based High Electron Mobility Transistors.* Materials (Basel) 2019, 12, 1599.

[2] Tolbert, L.M.; King, T.; Ozpineci, B.; Campbell, J.; Muralidharan, G.; Rizy, D.; Sabau, A.; Zhang, H.; Zhang, W.; Xu, Y.; et al. *Power Electronics for Distributed Energy Systems and Transmission and Distribution Applications: Assessing the Technical Needs for Utility Applications; U.S.* Department of Energy Office of Scientific and Technical Information: Washington, DC, USA, 2005.

[3] M. Spera, "Ohmic contacts on wide band gap semiconductors," PhD Thesis, CNR-IMM, ITALY, 2019.

[4] S. B. Bodzenta, *Thermal conductivity of AlN and AlN–GaN thin films deposited on Si and GaAs substrates,* Diamond and Related Materials, vol. 14, no. 10.1016/j.diamond.2005.01.016, pp. 1169-1174, 2005.